Available online at www.sciencedirect.com
SCIENCE DIRECT®
International Journal of Solids and Structures 42 (2005) 4278–4294
INTERNATIONAL JOURNAL OF SOLIDS and STRUCTURES
www.elsevier.com/locate/ijsolstr

High-frequency response of isotropic-laminated cylindrical shells modeled by a layer-wise theory

A.M.B. Braga *, Carlos E. Rivas A. *

Department of Mechanical Engineering, Pontificia Universidade Catolica do Rio de Janeiro, PUC-Rio, 22453-900 Rio de Janeiro, Brazil

Received 20 August 2003; received in revised form 14 June 2004

Abstract

In this paper, the high-frequency response of isotropic-laminated cylindrical shells is investigated using a layer-wise theory. The cylindrical shell is discretized in an arbitrary number of layers in the radial direction, and a three-dimensional stress state is assumed in each layer. Approximate numerical results obtained by the layer-wise theory are compared with the exact wave-dispersion analytical results. The very good agreement between approximate and exact results indicates that the layer-wise theory can accurately describe of the dynamic response of cylindrical shells in the high-frequency (short-wavelength) range.

Keywords: Laminated structures; Wave propagation; High frequency; Layer-wise theory; Cylindrical shells

1. Introduction

Various models have been developed to describe the mechanical behavior of thin cylindrical shells (Leissa, 1973). Classical theories do not, however, consider the effect of transverse stress or strain components, and therefore are inadequate for the dynamic analysis of thick shells or even thin shells in the high-frequency (short-wavelength) range. Higher-order shell theories, which take transverse shear into account, have often been employed to improve the response of classical theories. However, in the case of thick shells or when the analysis is made in the high-frequency range, their results are not always reliable (Reddy, 1989). Indeed, when the wavelengths of disturbances propagating in the shell are of the same order as its thickness, the usual polynomial interpolation of higher-order shell models can no longer accurately reproduce the through-thickness displacement fields. More so in the case of laminated shells. Reviews of different models

* Corresponding authors. Tel.: +55 21 3114 1181; fax: +55 21 3114 1165 (A.M.B. Braga).
E-mail addresses: abraga@mec.puc-rio.br (A.M.B. Braga), cerivaspe@yahoo.com (C.E. Rivas A.).

0020-7683/$ - see front matter
doi:10.1016/j.ijsolstr.2004.06.062

for shells, with particular emphasis on the proper treatment of transverse shear effects may be found in an article by Noor et al. (1996).

Layer-wise theories offer alternatives that were proven by many authors to be quite effective in handling thick composite shells. For instance, an approximate analysis based on the three-dimensional theory of elasticity was developed by Loy and Lam (1999), who used a layer-wise theory to study vibration of thick cylindrical shells. In another contribution, Huang and Dasgupta (1995) proposed a semi-analytical, three-dimensional, layer-wise theory to calculate natural frequencies of thick laminated composite cylindrical shells. Reddy and Teply (1991) employed a discrete-layer theory to investigate the buckling analysis of simply supported cross-ply cylindrical shells. Icardi (1998) proposed a *zig-zag* shell model capable of accurately predicting both the overall response and stress distributions of laminated shells. In order to study the active and sensory response of piezoelectric composites, Lee and Saravanos (2000) have employed layer-wise discretizations to interpolate both the electric potential and temperature fields while keeping a single-layer model for the displacement across the thickness of the laminated shell. Their mixed piezothermoelastic shell theory has been demonstrated to accurately represent the response of thin and moderately thick piezoelectric shells.

It is the objective of this paper to further assess the ability of a layer-wise theory to reproduce the response of cylindrical laminated shells in the high-frequency (short-wavelength) range. In particular, the present study employs a model based on Reddy's discrete layer-wise theory (Reddy and Teply, 1991). The displacements are interpolated in the through-thickness direction using piece-wise linear functions. The governing equations are formulated in the frequency domain and written in a state space form. The very good agreement obtained in comparisons between approximate and exact frequency spectra of guided waves propagating in an infinite, laminated, cylindrical shell, made of isotropic layers, show that the layer-wise theory is capable of simulating the dynamic response of cylindrical laminated shells in the high-frequency (short-wavelength) range. The solution of the state equation is obtained by employing an algorithm based on a discrete version of the Riccati transformation (Dieci et al., 1988; Braga et al., 2000). This algorithm is stable in a wide frequency range, even when the solution involves combinations of standing waves associated with real eigenvalues of the state matrix. As an example of application of the algorithm, the frequency response of a laminated cylindrical shell excited by an axi-symmetric, radial, co-localized load is evaluated and compared with similar results obtained with plane axi-symmetric finite elements of a commercial code.

2. Theoretical formulation

We employ a model based on the layer-wise theory of Reddy (see, e.g., Reddy and Robbins, 1994) to describe the response of a laminated cylindrical shell as show in Fig. 1. This structure is formed by an arbitrary number of perfectly bonded, elastic layers, each of uniform thickness. In each lamina a three-dimensional stress state is assumed. The variation, through the thickness, of the three-dimensional displacement field is assumed as follows:

$$\begin{aligned} u_r(r,\theta,z,t) &= \sum_{\alpha=1}^{N} \xi^{\alpha}(r) u_r^{\alpha}(\theta,z,t) \\ u_\theta(r,\theta,z,t) &= \sum_{\beta=1}^{M} \psi^{\beta}(r) u_\theta^{\beta}(\theta,z,t) \\ u_z(r,\theta,z,t) &= \sum_{\gamma=1}^{P} \eta^{\gamma}(r) u_z^{\gamma}(\theta,z,t) \end{aligned} \tag{1}$$

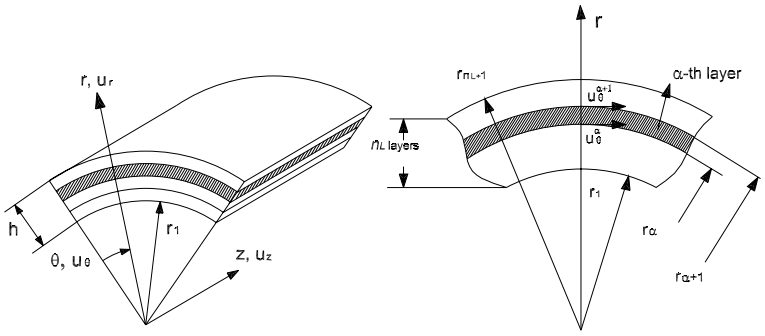

Fig. 1. Geometry of a cylindrical laminated shell.

In Reddy's layer-wise theory the interpolation functions ξ^{α}, ψ^{β}, η^{γ} are arbitrary. However, in this paper, we employ only linear Lagrange interpolation functions. Also, we consider the same number of interpolation functions ($N = M = P$) to represent the displacement field. We take $\alpha = \beta = \gamma = 1,2,\ldots,n_{\mathrm{L}},n_{\mathrm{L}}+1$, where n_{L} is the number of layers in the laminated shell. $u_r^{\alpha}, u_{\theta}^{\alpha}$ and u_z^{α} are, respectively, the displacements in the radial, circumferential, and axial direction between the layers $\alpha - 1$ and α. In this theory the number of subdivisions n_{L} does not necessarily has to coincide with the number of homogeneous layers. A homogeneous layer can be subdivided into two or more sub-layers increasing the number of interpolation functions. The interpolation functions are given by

$$\xi^{\alpha}(r) = \psi^{\alpha}(r) = \eta^{\alpha}(r) = \begin{cases} \dfrac{r_2 - r}{r_2 - r_1} & \text{if } r_1 < r < r_2 \ \ (\alpha = 1) \\ \dfrac{r - r_{\alpha-1}}{r_{\alpha} - r_{\alpha-1}} & \text{if } r_{\alpha-1} < r < r_{\alpha} \ \ (\alpha = 2,3,\ldots,n_{\mathrm{L}}) \\ \dfrac{r_{\alpha+1} - r}{r_{\alpha+1} - r_{\alpha}} & \text{if } r_{\alpha} < r < r_{\alpha+1} \ \ (\alpha = 2,3,\ldots,n_{\mathrm{L}}) \\ \dfrac{r - r_{n_{\mathrm{L}}}}{r_{n_{\mathrm{L}}+1} - r_{n_{\mathrm{L}}}} & \text{if } r_{n_{\mathrm{L}}} < r < r_{n_{\mathrm{L}}+1} \ \ (\alpha = n_{\mathrm{L}} + 1) \\ 0 & \text{otherwise} \end{cases} \tag{2}$$

The variational principle applied to the laminated cylindrical shell takes the form:

$$\int_V (T_1\delta S_1 + T_2\delta S_2 + T_3\delta S_3 + T_4\delta S_4 + T_5\delta S_5 + T_6\delta S_6)\,\mathrm{d}V + \int_V \rho\left(\frac{\partial^2 u_r}{\partial t^2}\delta u_r + \frac{\partial^2 u_\theta}{\partial t^2}\delta u_\theta + \frac{\partial^2 u_z}{\partial t^2}\delta u_z\right)\mathrm{d}V - \int_A (f_r\delta u_r)\,\mathrm{d}A = 0 \tag{3}$$

where f_r represent the external radial surface load. T_I and S_I ($I = 1,\ldots,6$) are the stress and strain components in cylindrical coordinates and ρ is the density of the cylindrical shell. The relation between the strain and the displacement components in cylindrical coordinates are given by

$$S_1 = \frac{\partial u_r}{\partial r} \quad S_2 = \frac{u_r}{r} + \frac{1}{r}\frac{\partial u_\theta}{\partial \theta} \quad S_3 = \frac{\partial u_z}{\partial z} \quad S_4 = \frac{\partial u_\theta}{\partial z} + \frac{1}{r}\frac{\partial u_z}{\partial_\theta} \quad S_5 = \frac{\partial u_r}{\partial z} + \frac{\partial u_z}{\partial r}$$
$$S_6 = \frac{1}{r}\frac{\partial u_r}{\partial \theta} + \frac{\partial u_\theta}{\partial r} - \frac{u_\theta}{r} \tag{4}$$

The constitutive equation for an orthotropic layer with material symmetry axes coinciding with the axial, circumferential, and radial directions, may be expressed as

$$\begin{bmatrix} T_1 \\ T_2 \\ T_3 \\ T_4 \\ T_5 \\ T_6 \end{bmatrix} = \begin{bmatrix} c_{11} & c_{12} & c_{13} & 0 & 0 & 0 \\ c_{12} & c_{22} & c_{23} & 0 & 0 & 0 \\ c_{13} & c_{23} & c_{33} & 0 & 0 & 0 \\ 0 & 0 & 0 & c_{44} & 0 & 0 \\ 0 & 0 & 0 & 0 & c_{55} & 0 \\ 0 & 0 & 0 & 0 & 0 & c_{66} \end{bmatrix} \begin{bmatrix} S_1 \\ S_2 \\ S_3 \\ S_4 \\ S_5 \\ S_6 \end{bmatrix} \tag{5}$$

For a isotropic layer:

$$c_{11} = c_{22} = c_{33} = \lambda + 2\mu \quad c_{12} = c_{13} = c_{23} = \lambda \quad c_{44} = c_{55} = c_{66} = \mu$$

where λ, μ are the Lamé's elastic constants. In order to simplify the variational Eq. (3) we define the following generalized forces:

$$P_i^\alpha = \int_{r_\alpha}^{r_{\alpha+1}} T_i \frac{\mathrm{d}\xi^\alpha(r)}{\mathrm{d}r} r \,\mathrm{d}r \quad i = 1, 5, 6 \tag{6}$$

$$T_i^\alpha = \int_{r_\alpha}^{r_{\alpha+1}} T_i \xi^\alpha(r) \,\mathrm{d}r \quad i = 2, 4, 6 \tag{7}$$

$$M_i^\alpha = \int_{r_\alpha}^{r_{\alpha+1}} T_i \xi^\alpha(r) r \,\mathrm{d}r \quad i = 3, 4, 5 \tag{8}$$

where r_α and $r_{\alpha+1}$ are, respectively, the inner and the outer radio of a homogeneous sub-lamina of the shell. Also we define the following quantities:

$$\begin{aligned} A^{\beta,\alpha}(c) &= \int_{r_\alpha}^{r_{\alpha+1}} c\xi^\beta(r)\xi^\alpha(r) r \,\mathrm{d}r & B^{\beta,\alpha}(c) &= \int_{r_\alpha}^{r_{\alpha+1}} c\xi^\beta(r)\xi^\alpha(r) \,\mathrm{d}r \\ C^{\beta,\alpha}(c) &= \int_{r_\alpha}^{r_{\alpha+1}} c\xi^\beta(r)\frac{\mathrm{d}\xi^\alpha(r)}{\mathrm{d}r} \,\mathrm{d}r & D^{\beta,\alpha}(c) &= \int_{r_\alpha}^{r_{\alpha+1}} c\frac{\xi^\beta(r)}{r}\xi^\alpha(r) \,\mathrm{d}r \\ E^{\beta,\alpha}(c) &= \int_{r_\alpha}^{r_{\alpha+1}} c\frac{\mathrm{d}\xi^\beta(r)}{\mathrm{d}r}\frac{\mathrm{d}\xi^\alpha(r)}{\mathrm{d}r} r \,\mathrm{d}r & F^{\beta,\alpha}(c) &= \int_{r_\alpha}^{r_{\alpha+1}} c\xi^\beta(r)\frac{\mathrm{d}\xi^\alpha(r)}{\mathrm{d}r} r \,\mathrm{d}r \end{aligned} \tag{9}$$

where c may represent any one of the mechanical properties of the layers.

From the variational principle in Eq. (3), and using the definitions in Eqs. (6)–(9), we obtain the following set of equations:

$$\frac{\partial}{\partial z}\begin{bmatrix} M_5^\alpha \\ M_4^\alpha \\ M_3^\alpha \end{bmatrix} + \frac{\partial}{\partial \theta}\begin{bmatrix} T_6^\alpha \\ T_2^\alpha \\ T_4^\alpha \end{bmatrix} = \begin{bmatrix} P_1^\alpha \\ P_6^\alpha \\ P_5^\alpha \end{bmatrix} + \begin{bmatrix} T_2^\alpha \\ -T_6^\alpha \\ 0 \end{bmatrix} + \sum_{\beta=1}^{N} \begin{bmatrix} A^{\beta,\alpha}(\rho) & 0 & 0 \\ 0 & A^{\beta,\alpha}(\rho) & 0 \\ 0 & 0 & A^{\beta,\alpha}(\rho) \end{bmatrix} \frac{\partial^2}{\partial t^2}\begin{bmatrix} u_r^\beta \\ u_\theta^\beta \\ u_z^\beta \end{bmatrix} + \begin{bmatrix} -f_r q^\alpha \\ 0 \\ 0 \end{bmatrix} \tag{10}$$

where $q^\alpha = 0$, except for $\alpha = N = n_\mathrm{L} + 1$ when $q^\alpha = r_{n_\mathrm{L}+1}$ (outer radius).

We are interested in the harmonic response of the cylindrical shell, so a generic function $F(r, \theta, z, t)$ can be written in the form:

$$F(r, \theta, z, t) = F_n(r, z)\, \mathrm{e}^{\mathrm{i}(n\theta - \omega t)} \tag{11}$$

Using the above assumption, Eqs. (6)–(8) can be rewritten as:

$$P_i^\alpha = p_i^\alpha(z)\, \mathrm{e}^{\mathrm{i}(n\theta - \omega t)} \tag{12}$$

$$T_i^\alpha = t_i^\alpha(z)\, \mathrm{e}^{\mathrm{i}(n\theta - \omega t)} \tag{13}$$

$$M_i^\alpha = m_i^\alpha(z)\,\mathrm{e}^{\mathrm{i}(n\theta-\omega t)} \tag{14}$$

Now, Eq. (10) can be rewritten using Eqs. (11)–(14). Therefore:

$$\frac{\mathrm{d}}{\mathrm{d}z}\begin{bmatrix} m_5^\alpha \\ m_4^\alpha \\ m_3^\alpha \end{bmatrix} + in\begin{bmatrix} t_6^\alpha \\ t_2^\alpha \\ t_4^\alpha \end{bmatrix} = \begin{bmatrix} p_1^\alpha \\ p_6^\alpha \\ p_5^\alpha \end{bmatrix} + \begin{bmatrix} t_2^\alpha \\ -t_6^\alpha \\ 0 \end{bmatrix} - \omega^2 \sum_{\beta=1}^{N} \underbrace{\begin{bmatrix} A^{\beta,\alpha}(\rho) & 0 & 0 \\ 0 & A^{\beta,\alpha}(\rho) & 0 \\ 0 & 0 & A^{\beta,\alpha}(\rho) \end{bmatrix}}_{\mathbf{U}_0} \begin{bmatrix} u_r^\beta \\ u_\theta^\beta \\ u_z^\beta \end{bmatrix} + \underbrace{\begin{bmatrix} -f_r q^\alpha \\ 0 \\ 0 \end{bmatrix}}_{\mathbf{F}_0} \tag{15}$$

Also, Eqs. (12)–(14) are rewritten using the constitute equations (5) yielding:

$$\begin{bmatrix} m_5^\alpha \\ m_4^\alpha \\ m_3^\alpha \end{bmatrix} = \sum_{\beta=1}^{N} \underbrace{\begin{bmatrix} 0 & 0 & F^{\alpha,\beta}(c_{55}) \\ 0 & 0 & inB^{\beta,\alpha}(c_{44}) \\ F^{\alpha,\beta}(c_{13}) + B^{\beta,\alpha}(c_{23}) & inB^{\beta,\alpha}(c_{23}) & 0 \end{bmatrix}}_{\mathbf{U}_1} \begin{bmatrix} u_r^\beta \\ u_\theta^\beta \\ u_z^\beta \end{bmatrix} + \sum_{\beta=1}^{N} \underbrace{\begin{bmatrix} A^{\beta,\alpha}(c_{55}) & 0 & 0 \\ 0 & A^{\beta,\alpha}(c_{44}) & 0 \\ 0 & 0 & A^{\beta,\alpha}(c_{33}) \end{bmatrix}}_{\mathbf{V}_1} \frac{\mathrm{d}}{\mathrm{d}z}\begin{bmatrix} u_r^\beta \\ u_\theta^\beta \\ u_z^\beta \end{bmatrix} \tag{16}$$

$$\begin{bmatrix} t_6^\alpha \\ t_2^\alpha \\ t_4^\alpha \end{bmatrix} = \sum_{\beta=1}^{N} \underbrace{\begin{bmatrix} inD^{\beta,\alpha}(c_{66}) & C^{\alpha,\beta}(c_{66}) - D^{\beta,\alpha}(c_{66}) & 0 \\ C^{\alpha,\beta}(c_{12}) + D^{\beta,\alpha}(c_{22}) & inD^{\beta,\alpha}(c_{22}) & 0 \\ 0 & 0 & inD^{\beta,\alpha}(c_{44}) \end{bmatrix}}_{\mathbf{U}_2} \begin{bmatrix} u_r^\beta \\ u_\theta^\beta \\ u_z^\beta \end{bmatrix} + \sum_{\beta=1}^{N} \underbrace{\begin{bmatrix} 0 & 0 & 0 \\ 0 & 0 & B^{\beta,\alpha}(c_{23}) \\ 0 & B^{\beta,\alpha}(c_{44}) & 0 \end{bmatrix}}_{\mathbf{V}_2} \frac{\mathrm{d}}{\mathrm{d}z}\begin{bmatrix} u_r^\beta \\ u_\theta^\beta \\ u_z^\beta \end{bmatrix} \tag{17}$$

$$\begin{bmatrix} p_1^\alpha \\ p_6^\alpha \\ p_5^\alpha \end{bmatrix} = \sum_{\beta=1}^{N} \underbrace{\begin{bmatrix} E^{\beta,\alpha}(c_{11}) + C^{\beta,\alpha}(c_{12}) & inC^{\beta,\alpha}(c_{12}) & 0 \\ inC^{\beta,\alpha}(c_{66}) & E^{\beta,\alpha}(c_{66}) - C^{\beta,\alpha}(c_{66}) & 0 \\ 0 & 0 & E^{\beta,\alpha}(c_{55}) \end{bmatrix}}_{\mathbf{U}_3} \begin{bmatrix} u_r^\beta \\ u_\theta^\beta \\ u_z^\beta \end{bmatrix} + \sum_{\beta=1}^{N} \underbrace{\begin{bmatrix} 0 & 0 & F^{\beta,\alpha}(c_{13}) \\ 0 & 0 & 0 \\ F^{\beta,\alpha}(c_{55}) & 0 & 0 \end{bmatrix}}_{\mathbf{V}_3} \frac{\mathrm{d}}{\mathrm{d}z}\begin{bmatrix} u_r^\beta \\ u_\theta^\beta \\ u_z^\beta \end{bmatrix} \tag{18}$$

$$\begin{bmatrix} t_2^\alpha \\ -t_6^\alpha \\ 0 \end{bmatrix} = \sum_{\beta=1}^{N} \underbrace{\begin{bmatrix} C^{\alpha,\beta}(c_{12}) + D^{\beta,\alpha}(c_{22}) & inD^{\beta,\alpha}(c_{22}) & 0 \\ -inD^{\beta,\alpha}(c_{66}) & D^{\beta,\alpha}(c_{66}) - C^{\alpha,\beta}(c_{66}) & 0 \\ 0 & 0 & 0 \end{bmatrix}}_{\mathbf{U_4}} \begin{bmatrix} u_r^\beta \\ u_\theta^\beta \\ u_z^\beta \end{bmatrix}$$
$$+ \sum_{\beta=1}^{N} \underbrace{\begin{bmatrix} 0 & 0 & B^{\beta,\alpha}(c_{23}) \\ 0 & 0 & 0 \\ 0 & 0 & 0 \end{bmatrix}}_{\mathbf{V_4}} \frac{\mathrm{d}}{\mathrm{d}z} \begin{bmatrix} u_r^\beta \\ u_\theta^\beta \\ u_z^\beta \end{bmatrix} \tag{19}$$

By applying Eqs. (16)–(19) in Eq. (15), and after some manipulation we obtain the state equation:

$$\frac{\mathrm{d}\boldsymbol{\zeta}}{\mathrm{d}z} = \mathbf{A}\boldsymbol{\zeta} + \mathbf{F} \tag{20}$$

where $\mathbf{F}$ is the distributed load vector defined as:

$$\mathbf{F} = \begin{bmatrix} 0 \\ \mathbf{F_0} \end{bmatrix} \tag{21}$$

The state vector $\boldsymbol{\zeta}$, and the state matrix $\mathbf{A}$ are defined as:

$$\zeta = \begin{bmatrix} \mathbf{u} \\ \mathbf{m} \end{bmatrix} \quad \mathbf{A} = \begin{bmatrix} \mathbf{A_{11}} & \mathbf{A_{12}} \\ \mathbf{A_{21}} & \mathbf{A_{22}} \end{bmatrix} \tag{22}$$

with

$$\mathbf{u} = \begin{bmatrix} \mathbf{u_r} \\ \mathbf{u}_\theta \\ \mathbf{u_z} \end{bmatrix} \quad \mathbf{m} = \begin{bmatrix} \mathbf{m_5} \\ \mathbf{m_4} \\ \mathbf{m_3} \end{bmatrix} \tag{23}$$

and

$$\mathbf{A_{11}} = -\mathbf{V_1^{-1}U_1} \quad \mathbf{A_{12}} = \mathbf{V_1^{-1}} \quad \mathbf{A_{21}} = \mathbf{N_2} + \mathbf{N_1V_1^{-1}U_1} \quad \mathbf{A_{22}} = -\mathbf{N_1V_1^{-1}} \tag{24}$$

$\mathbf{u_r}$, $\mathbf{u}_\theta$, $\mathbf{u_z}$ are vectors of dimension $n_L + 1$ grouping the variables $u_r^\beta, u_\theta^\beta, u_z^\beta$. $\mathbf{m_5}$, $\mathbf{m_4}$, $\mathbf{m_3}$ are generalized forces, also of dimension $n_L + 1$ defined in Eq. (14). The matrices $\mathbf{N_1}$ and $\mathbf{N_2}$ take the form:

$$\mathbf{N_1} = in\mathbf{V_2} - \mathbf{V_3} - \mathbf{V_4} \quad \mathbf{N_2} = \mathbf{U_3} + \mathbf{U_4} - in\mathbf{U_2} - \omega^2\mathbf{U_0} \tag{25}$$

The state equation (20) describes the harmonic response of the laminated cylindrical shell. The state matrix $\mathbf{A}$ depends on the circumferential harmonic n, the frequency ω, and the number of homogeneous layers n_L.

3. Exact frequency spectrum

3.1. Homogeneous media

In cylindrical coordinates, the displacement field in a homogeneous isotropic body can be written in the form:

$$\mathbf{u} = \nabla\varphi + \nabla \times (\chi\mathbf{e_z}) + \nabla \times (\eta\mathbf{e_z}) \tag{26}$$

In this equation $\mathbf{e_z}$ is a unit vector in the axial direction, and the scalar potentials φ, χ and η satisfy the wave equations:

$$\nabla^2\varphi = \frac{1}{c_L^2}\frac{\partial^2\varphi}{\partial t^2} \quad \text{and} \quad \nabla^2\begin{Bmatrix}\chi\\ \eta\end{Bmatrix} = \frac{1}{c_T^2}\frac{\partial^2}{\partial t^2}\begin{Bmatrix}\chi\\ \eta\end{Bmatrix} \tag{27}$$

where c_L and c_T are the speeds of longitudinal and transverse waves respectively.

At this point we introduce the three-dimensional array of scalar potentials $\boldsymbol{\phi}$, defined as:

$$\boldsymbol{\phi} = \begin{Bmatrix}\varphi\\ \chi\\ \eta\end{Bmatrix} \tag{28}$$

Considering harmonic motions of the form:

$$\boldsymbol{\phi} = \overline{\boldsymbol{\phi}}(r)\,e^{i(n\theta+k_z z-\omega t)} \tag{29}$$

$$\mathbf{u} = \overline{\mathbf{u}}(r)\,e^{i(n\theta+k_z z-\omega t)} \tag{30}$$

$$\mathbf{t} = \overline{\mathbf{t}}(r)\,e^{i(n\theta+k_z z-\omega t)} \tag{31}$$

where $\mathbf{t}$ is the traction vector acting across a surface normal to the radial direction, and k_z is the wave-number in the axial direction.

Using the above assumption, Eqs. (27) can be solved, yielding:

$$\overline{\boldsymbol{\phi}}(r) = \sum_{\alpha=1}^{2}\boldsymbol{\Phi}_\alpha(r)\mathbf{c}_\alpha \tag{32}$$

where

$$\boldsymbol{\Phi}_\alpha(r) = \mathrm{diag}(H_n^\alpha(k_L r), H_n^\alpha(k_T r), H_n^\alpha(k_T r)), \quad \alpha = 1,2 \tag{33}$$

and $\mathbf{c}_\alpha$ is the three-dimensional array of constants, while k_j $(j = L, T)$ represent the wave-number in the longitudinal and transverse directions, respectively. In Eqs. (33), $H_n^\alpha(x)$ are the Hankel functions (Abramowitz and Stegun, 1972).

From Eqs. (32) and (26), we obtain the displacement field in cylindrical coordinates:

$$\overline{\mathbf{u}}(r) = \sum_{\alpha=1}^{2}\underline{\boldsymbol{A}}_\alpha(r)\boldsymbol{\tau}_\alpha(r)\mathbf{c}_\alpha \tag{34}$$

where

$$\boldsymbol{\tau}_1(r) = \mathrm{diag}(e^{ik_L r}, e^{ik_T r}, e^{ik_T r}), \tag{35}$$

and

$$\boldsymbol{\tau}_2(r) = \boldsymbol{\tau}_1^{-1}(r) \tag{36}$$

The traction vector $\overline{\mathbf{t}}(r)$ is obtained by substituting Eq. (34) in the elastic stress–strain relation for isotropic media in cylindrical coordinates. In matrix form, we can write the traction field as:

$$\overline{\mathbf{t}}(r) = \sum_{\alpha=1}^{2}\underline{\boldsymbol{L}}_\alpha(r)\boldsymbol{\tau}_\alpha(r)\mathbf{c}_\alpha \tag{37}$$

The components of the matrices $\underline{\boldsymbol{A}}_\alpha(r)$ contain the Hankel functions of Eq. (33) scaled by complex exponentials. Both matrices, $\underline{\boldsymbol{A}}_\alpha(r)$ and $\underline{\boldsymbol{L}}_\alpha(r)$ can be found in the article by Braga et al. (1990).

In these equations, the quantities with the subscript $\alpha = 1$ are associated with partial waves that propagate radially outward (outgoing waves), while partial waves propagating in the opposite direction (incoming waves), are represented by quantities with $\alpha = 2$. In this way, we can write the displacement field and the traction vector as:

$$\bar{\mathbf{u}}(r) = \bar{\mathbf{u}}_1(r) + \bar{\mathbf{u}}_2(r) \tag{38}$$

$$\bar{\mathbf{t}}(r) = \bar{\mathbf{t}}_1(r) + \bar{\mathbf{t}}_2(r) \tag{39}$$

where

$$\bar{\mathbf{u}}_\alpha(r) = \mathbf{M}_\alpha(r, r_0)\bar{\mathbf{u}}_\alpha(r_0) \tag{40}$$

$$\bar{\mathbf{t}}_\alpha(r) = -\mathrm{i}\omega\mathbf{Z}_\alpha(r)\bar{\mathbf{u}}_\alpha(r) \tag{41}$$

with

$$\mathbf{M}_\alpha(r, r_0) = \underline{\boldsymbol{A}}_\alpha(r)\boldsymbol{\tau}_\alpha(r - r_0)\underline{\boldsymbol{A}}_\alpha^{-1}(r_0) \tag{42}$$

$$\mathbf{Z}_\alpha(r) = \frac{\mathrm{i}}{\omega}\underline{\boldsymbol{L}}_\alpha(r)\underline{\boldsymbol{A}}_\alpha^{-1}(r) \tag{43}$$

The matrices $\mathbf{M}_\alpha(r,r_0)$ relate the displacement field associated with the outgoing ($\alpha = 1$), or incoming ($\alpha = 2$), wave at the radial coordinate r with its value at r_0. The operator $\mathbf{Z}_\alpha(r)$ is the local impedance of the homogeneous solid, relating the traction with the velocity field across a cylindrical surface of radius r_0. We also observe that

$$\mathbf{M}_\alpha^{-1}(r, r_0) = \mathbf{M}_\alpha(r_0, r) \quad \text{and} \quad \mathbf{M}_\alpha(r_0, r_0) = \mathbf{I} \tag{44}$$

3.2. The surface impedance of a cylindrical layer

For an infinite cylinder as shown in Fig. 2, $\mathbf{G}_0$ and $\mathbf{G}_1$ represent the impedance tensor along its inner (r_0) and outer (r_1) radius, respectively. If the interior surface of the layer is traction free, we let $\mathbf{G}_0 = 0$. At $r = r_0$, we have:

$$\bar{\mathbf{t}}(r_0) = -\mathrm{i}\omega\mathbf{G}_0\bar{\mathbf{u}}(r_0) \tag{45}$$

Here, the generalized reflection tensor, which relates the incoming and outgoing fields everywhere, is defined. At the cylindrical surface $r = r_0$ the reflection tensor is denoted by $\mathbf{R}_0$ and defined by the following expression

$$\bar{\mathbf{u}}_1(r_0) = \mathbf{R}_0\bar{\mathbf{u}}_2(r_0) \tag{46}$$

Combining this equation with Eqs. (38) and (39) we obtain

$$\bar{\mathbf{t}}(r_0) = -\mathrm{i}\omega[\mathbf{Z}_1(r_0)\mathbf{R}_0 + \mathbf{Z}_2(r_0)](\mathbf{R}_0 + \mathbf{I})^{-1}\bar{\mathbf{u}}(r_0) \tag{47}$$

Comparing Eqs. (45) and (47), we can get the reflection tensor at the inner radius

$$\mathbf{R}_0 = [\mathbf{Z}_1(r_0) - \mathbf{G}_0]^{-1}[\mathbf{G}_0 - \mathbf{Z}_2(r_0)] \tag{48}$$

The generalized reflection tensor is obtained by combining Eqs. (46) and (40):

$$\bar{\mathbf{u}}_1(r) = \mathbf{H}(r)\bar{\mathbf{u}}_2(r) \quad r_0 < r < r_1 \tag{49}$$

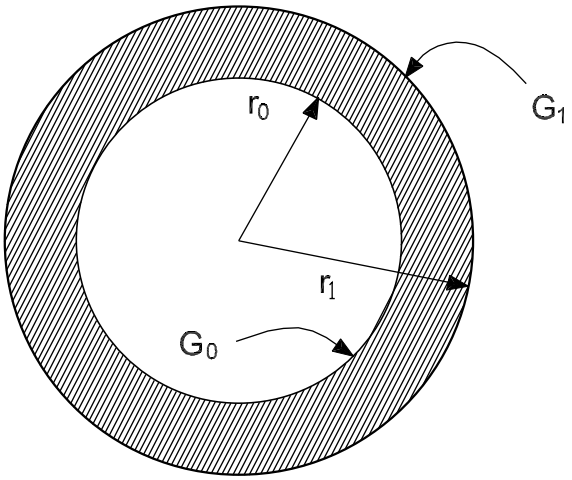

Fig. 2. Homogeneous isotropic cylindrical layer.

where

$$\mathbf{H}(r) = \mathbf{M}_1(r, r_0)\mathbf{R}_0\mathbf{M}_2(r_0, r) \tag{50}$$

Similarly to Eq. (45), at $r = r_1$ we have:

$$\bar{\mathbf{t}}(r_1) = -\mathrm{i}\omega\mathbf{G}_1\bar{\mathbf{u}}(r_1) \tag{51}$$

where $\mathbf{G}_1$ is the surface impedance tensor of the cylindrical layer, given by

$$\mathbf{G}_1 = [\mathbf{Z}_1(r_1)\mathbf{H}(r_1) + \mathbf{Z}_2(r_1)][\mathbf{I} + \mathbf{H}(r_1)]^{-1} \tag{52}$$

3.3. The surface impedance of laminated cylindrical shells

The results of the preceding sub-section are generalized to calculate the surface impedance of a laminated cylindrical shell made of m isotropic layers as shown in Fig. 3. The surface impedance $\mathbf{G_m}$ is obtained recursively using the following algorithm

Given $\mathbf{G}_0$, k_z, n, $e\omega$

For $j = 1$ to m Repeat

$$\mathbf{R}_{j-1} = -\left[\mathbf{Z}_1^{(j)}(r_{j-1}) - \mathbf{G}_{j-1}\right]^{-1}\left(\mathbf{Z}_2^{(j)}(r_{j-1}) - \mathbf{G}_{j-1}\right)$$

$$\mathbf{H}(r_j) = \mathbf{M}_1^{(j)}(r_j, r_{j-1})\mathbf{R}_{j-1}\mathbf{M}_2^{(j)}(r_{j-1}, r_j)$$

$$\mathbf{G}_j = \left[\mathbf{Z}_1^{(j)}(r_j)\mathbf{H}(r_j) + \mathbf{Z}_2^{(j)}(r_j)\right]\left[\mathbf{I} + \mathbf{H}(r_j)\right]^{-1}$$

End

In the last layer, we can write:

$$\bar{\mathbf{t}}(r_m) = -\mathrm{i}\omega\mathbf{G}_m\bar{\mathbf{u}}(r_m) \tag{53}$$

We now consider a traction-free laminated cylinder, that is, $\bar{\mathbf{t}}(r_m) = 0$. Free guided waves propagate in the shell for those combinations of the axial wave-number, k_z, circumferential harmonic, n, and frequency, ω, that satisfy the following equation:

$$\det(\mathbf{G}_m) = 0 \tag{54}$$

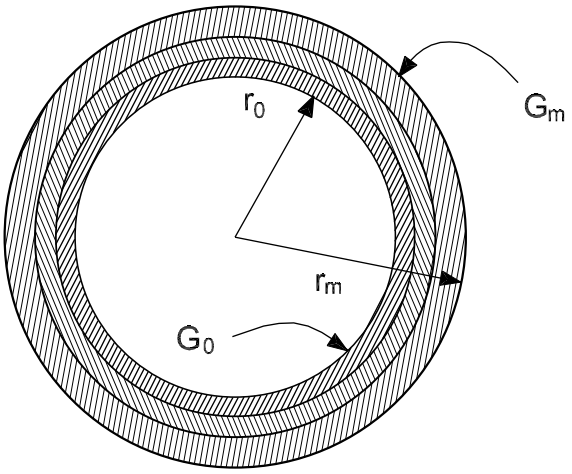

Fig. 3. Laminated cylindrical shell.

Hence, zeros of the function $\mathbf{G}_m(\omega, k_z, n)$ generate the frequency spectrum of guided waves that propagate freely in the infinite laminated cylinder. For a given circumferential harmonic, n, the spectrum is represented by curves generated by those pairs (ω, k_z) that make the surface impedance tensor to be singular. These are dispersion curves of the guided waves in the cylindrical shell.

4. Validation of the approximate theory

The high-frequency response predicted by the approximate model is assessed in this section by comparing frequency spectra of free guided waves propagating in an infinite laminated shell, calculated by both the layer-wise theory and the exact analysis described in the preceding section. The approximate frequency spectrum can be easily evaluated from the state matrix in Eq. (20). In fact, for a given frequency, ω, and circumferential harmonic, n, the wave-numbers of guided waves that propagate freely in the cylindrical laminate are directly related to the eigenvalues of the state matrix. If an eigenvalue of the state matrix $\mathbf{A}$, denoted as $-ik_z$, is complex, it represents an attenuated standing wave. If $-ik_z$ is pure imaginary or pure real, it either represents, respectively, a propagating or a near-field standing wave.

Fig. 5 shows a comparison between exact and approximate guided wave frequency spectra for an infinite, homogeneous, isotropic cylindrical shell of steel, as can be seen in Fig. 4(a). Results are for $n = 1$ and a shell with outer radius to thickness ratio equal to 11 ($R/h = 11$). The shell was divided into 10 homogeneous layers of equal thickness ($n_L = 10$). Only dispersion curves for propagating waves, with real wave-numbers ($\Im(k_z) = 0$), are depicted. We recall that those waves are associated with pure imaginary eigenvalues of the state matrix in Eq. (20). Curves are plotted in terms of the thickness to wavelength ratio (h/λ). We observe that the agreement between approximate and exact dispersion curves are excellent, up to wavelengths that are closely to 40% shorter than the shell thickness.

Fig. 6 shows the same comparison for a laminated cylindrical shell composed of three homogeneous, equally thick, layers of steel, aluminum, and copper as shown in Fig. 4(b). In this case, the thickness of each one of the three homogeneous layers were divided into 10 sub-layers of equal thickness. The number of interpolation functions in the layer-wise model was then $n_L + 1 = 31$. In this case results are for the circumferential harmonic $n = 0$, and only propagating waves are depicted. The laminated shell has an outer radius

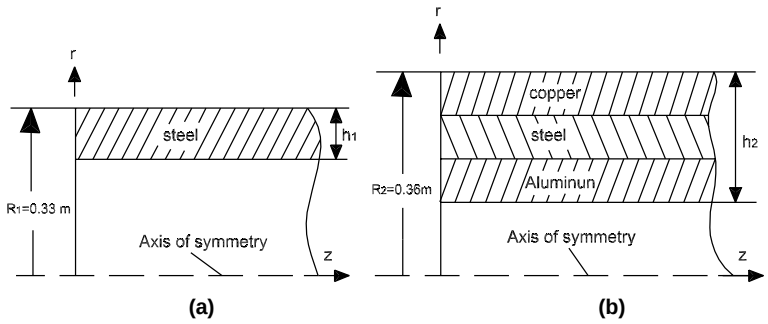

Fig. 4. Section of two cylindrical shells ($R_1/h_1 = 11, R_2/h_2 = 6$).

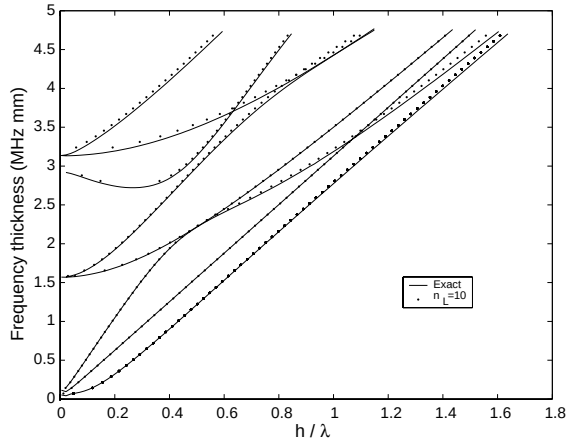

Fig. 5. Frequency spectrum of an isotropic cylinder ($n = 1$, $R/h = 11$).

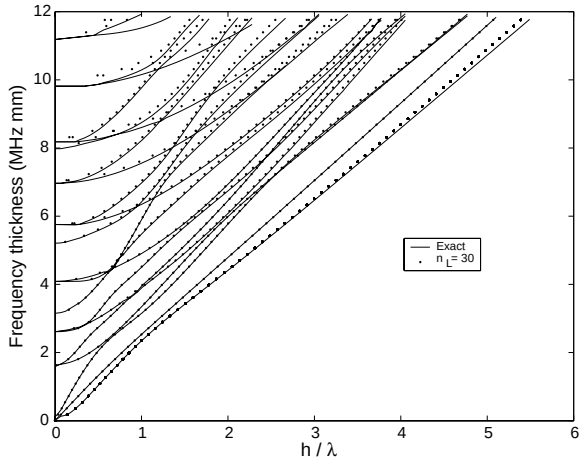

Fig. 6. Frequency spectrum of a laminated cylinder ($n = 0$, $R/h = 6$).

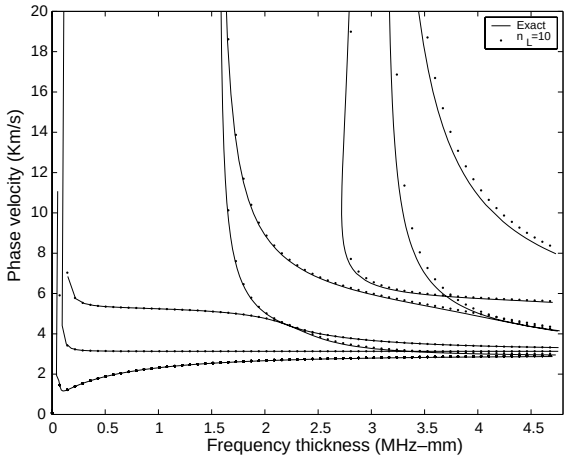

Fig. 7. Dispersion curve for an isotropic cylinder ($n = 1$, $R/h = 11$).

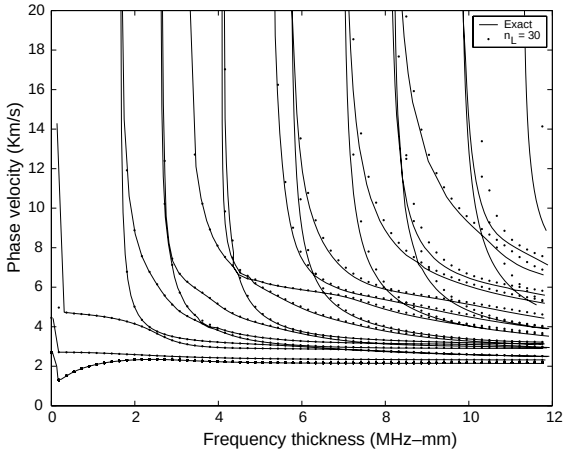

Fig. 8. Dispersion curve for a laminated cylinder ($n = 0$, $R/h = 6$).

to thickness ratio equal to 6 ($R/h = 6$). The agreement between approximate and exact dispersion curves is again very good. Now, up to wavelengths that are, at least, 80% shorter than the shell thickness.

We also show, in Figs. 7 and 8, the same results depicted in Figs. 5 and 6, but now presented in terms of the wave-speed rather than the wavelength. All results presented in this section clearly indicate that the

Table 1
Mechanical properties for isotropic materials ($\overline{\rho} = 2700$ Kg/m^3, $\overline{\mu} = 2.5947 \times 10^{10}$ Pa, e $\overline{c} = 3100$ m/s)

	$\frac{\rho}{\overline{\rho}}$	$\frac{\lambda}{\overline{\mu}}$	$\frac{\mu}{\overline{\mu}}$	$\frac{c_L}{\overline{c}}$	$\frac{c_T}{\overline{c}}$
Aluminum	1	2.13	1	2.03	1
Steel	2.88	4.29	2.86	1.86	0.99
Copper	3.29	3.62	1.81	1.48	0.74

layer-wise model, based on Reddy's theory (Reddy and Teply, 1991), is capable of accurately describing the shell response in the short-wavelength range. The mechanical properties of the isotropic materials used in this paper can be found in Table 1.

5. Solution of the state equation

For a proper set of boundary conditions, solutions for the state equation developed in Section 2, Eq. (20), provide approximate representations of the dynamic response of laminated cylindrical shells. We verified in the preceding section that these approximate representations may be accurate in a wide frequency range, even for wavelengths that are much shorter than the shell thickness.

The same approach employed to obtain the exact solution for guided waves in the cylindrical shell, described in Section 3, can be applied to the approximate theory. Again, after the proper transformations, namely when harmonic fields, both in time and in the circumferential direction, are considered, the problem becomes one-dimensional. While in Section 3 we were concerned with the exact solution in the radial direction, now, for the approximated problem, we need to obtain the generalized displacements and forces distributions along the axial direction. Furthermore, in Section 3, we were able to obtain part of the exact solution—concerning free, guided waves—only in the case of an infinite cylindrical shell. We now consider a finite shell, and must take into account boundary conditions at both ends.

The method we propose to solve Eq. (20) is based on a discrete version of the Riccati transformation, which provides an effective way to solve two-point boundary value problems that present exponential dichotomy (Dieci et al., 1988). The exponential dichotomy is related to the fact that the eigenvalues of the state matrix in Eq. (20) always appear in pairs of opposite signs. Indeed, this is a consequence of the following property of this matrix (Pease, 1965):

$$\mathbf{T}\mathbf{A}\mathbf{T}^T = -\mathbf{A}^T \quad \text{where } \mathbf{T} = \begin{bmatrix} 0 & \mathbf{I} \\ -\mathbf{I} & 0 \end{bmatrix} \tag{55}$$

where $\mathbf{I}$ denotes the identity matrix.

The problem with the exponential dichotomy arises in the high-frequency range, when some of the eigenvalues of $\mathbf{A}$ have large real parts with opposite signs, resulting in rapidly decaying as well as growing exponentials (Chin et al., 1984). These are associated with standing waves attenuated in both senses along the axial direction. The solution scheme proposed here, isolates the rapidly growing exponential solutions, which are never computed. This is accomplished, firstly, by the following decomposition of the state matrix:

$$\mathbf{A} = \begin{bmatrix} \mathbf{A_1} & \mathbf{A_2} \\ \mathbf{L_1} & \mathbf{L_2} \end{bmatrix} \begin{bmatrix} \mathbf{\Lambda} & 0 \\ 0 & -\mathbf{\Lambda} \end{bmatrix} \begin{bmatrix} \mathbf{A_1} & \mathbf{A_2} \\ \mathbf{L_1} & \mathbf{L_2} \end{bmatrix}^{-1} \tag{56}$$

where $\mathbf{\Lambda}$ is a diagonal matrix containing the eigenvalues of $\mathbf{A}$ whose real part is negative or, if purely imaginary, whose imaginary part is positive. These are the eigenvalues related to guided waves that propagate or are attenuated in the positive axial direction. $\mathbf{A_1}$, $\mathbf{A_2}$, $\mathbf{L_1}$, $\mathbf{L_2}$ are matrices obtained after regrouping the eigenvectors according to the position of their eigenvalues.

In order to proceed, we further introduce the following matrices:

$$\begin{aligned} &\mathbf{k_1} = \mathbf{A_1}\mathbf{\Lambda}\mathbf{A_1^{-1}}, && \mathbf{k_2} = -\mathbf{A_2}\mathbf{\Lambda}\mathbf{A_2^{-1}} \\ &\mathbf{M_1}(z) = \mathrm{e}^{\mathbf{k_1}z}, && \mathbf{M_2}(z) = \mathrm{e}^{\mathbf{k_2}z} \\ &\mathbf{Z_1} = \tfrac{\mathrm{i}}{\omega}\mathbf{L_1}\mathbf{A_1^{-1}}, && \mathbf{Z_2} = \tfrac{\mathrm{i}}{\omega}\mathbf{L_2}\mathbf{A_2^{-1}} \\ &\mathbf{H}(z) = \mathbf{M_1}(z)\mathbf{R}_1\mathbf{M_2^{-1}}(z), && \mathbf{G}_2(z) = [\mathbf{Z_1}\mathbf{H}(z) + \mathbf{Z_2}][\mathbf{H}(z) + \mathbf{I}]^{-1} \end{aligned} \tag{57}$$

where $\mathbf{R_1}$ is a reflection matrix, and $\mathbf{G_2}$ an impedance matrix. The first is defined at the left-end of the cylinder ($z = 0$), and the second at its right-end. The impedance matrix relates generalized forces with generalized particles velocities. The matrix $\mathbf{H}(z)$ relates the group of propagating, or attenuated, partial waves in the negative axial direction with those of opposite sense. It is this matrix that may be associated with a Riccati transformation (Dieci et al., 1988). We observe that the growing exponentials are associated with matrix $\mathbf{M}_2(z)$ in (57). As in Section 3, we assume that the impedance matrix at the left-end of the shell, $\mathbf{G_1}$, is known. For example, if the left boundary is free, we take $\mathbf{G_1} = 0$, whereas if the cylinder is clamped, we let $\mathbf{G_1}^{-1} = 0$. Between these two limits there are various possibilities.

We now consider a cylindrical shell as schematically shown in Fig. 9. The laminated shell is formed by N pieces, which may be composed by different or equal numbers of layers. The interfaces between pieces are labelled by j, running from 1 to $N+1$ as is shown in the Fig. 9. Concentrated, generalized forces may be applied at the interfaces. A laminated shell may be sub-divided in an arbitrary number of pieces.

The following algorithm, similar to that presented in Section 3, is proposed to obtain the solution. In this algorithm the superscripts indicate the position of a homogeneous piece of the cylinder, and the subscripts indicate the interfaces. f_I represents a concentrated, generalized force applied at interface I.

For ω, $\mathbf{G_1}$, n, and f_1 given:

Repeat from $j = 1$ to N:

$$\mathbf{R_j} = -(\mathbf{Z}_1^j - \mathbf{G_j})^{-1}(\mathbf{Z}_2^j - \mathbf{G_j})$$
$$\mathbf{S_j} = -\tfrac{\mathrm{i}}{\omega}(\mathbf{Z}_1^j - \mathbf{G_j})^{-1}$$
$$\mathbf{H_{j+1}} = \mathbf{M}_1^j(\mathbf{L_j})\mathbf{R_j}(\mathbf{M}_2^j(\mathbf{L_j}))^{-1}$$
$$\mathbf{G_{j+1}} = (\mathbf{Z}_1^j\mathbf{H_{j+1}} + \mathbf{Z}_2^j)(\mathbf{H_{j+1}} + \mathbf{I})^{-1}$$
$$\mathbf{h_{j+1}} = -\mathrm{i}\omega(\mathbf{G_{j+1}} - \mathbf{Z}_1^j)\mathbf{M}_1^j(\mathbf{L_j})$$
$$\mathbf{f_{j+1}} = -\mathbf{h_{j+1}}\mathbf{f_j} - \mathbf{f_{j+1}}$$

End

At the right end of the cylinder we find the following relationship:

$$\mathbf{m_{N+1}} = -\mathrm{i}\omega\mathbf{G_{N+1}}\mathbf{u_{N+1}} - \mathbf{f_{N+1}} \tag{58}$$

where $\mathbf{m_{N+1}}$ and $\mathbf{u_{N+1}}$ are the generalized force and displacement at the right end.

In order to determine the displacement field through the thickness at any interface we have to march backwards:

Repeat from $j = N$ to 1

$$\mathbf{u_{2(j+1)}} = (\mathbf{I} + \mathbf{H_{j+1}})^{-1}(\mathbf{u_{j+1}} - \mathbf{M}_1^j(\mathbf{L_j})\mathbf{S_j}\mathbf{f_j})$$
$$\mathbf{u_j} = (\mathbf{I} + \mathbf{R_j})(\mathbf{M}_2^j(\mathbf{L_j}))^{-1}\mathbf{u_{2(j+1)}} + \mathbf{S_j}\mathbf{f_j}$$

End

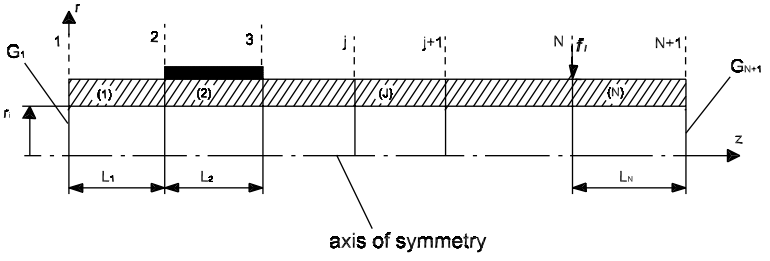

Fig. 9. Non-homogeneous laminated cylinder.

This algorithm, based on a discrete version of the Riccati transformation, is very stable in the high-frequency range. The key point is that only the inverse of matrix $\mathbf{M_2}(z)$, that contains rapidly growing exponentials, is evaluated. Hence, the computation of growing exponentials associated with the positive real eigenvalues of $\mathbf{A}$ is avoided.

As an application example of the algorithm, we present results concerning the frequency response of a laminated cylindrical shell, clamped at its left-boundary and excited, at the other end, by an axi-symmetric, radial distributed load as can be seen in Fig. 10. In this case, we divided the thickness of each isotropic layer in 10 sub-layers of equal thickness ($n_L = 30$).

Fig. 11 shows, how the radial displacement at the point were the load is applied varies with the frequency of excitation. Results have been compared with those obtained by employing plane axi-symmetric finite elements of the commercial code ANSYS 5.5. The FEM solution was obtained meshing the section of the laminated cylinder with 7500 square, axi-symmetric, plane elements distributed as shown in the Fig. 12. When comparing both results, one should consider the data presented in Section 4, in particular in Fig. 6. It was shown there that the layer-wise theory is capable of accurately reproducing the frequency spectra of guided waves propagating in the shell of Fig. 10 up to frequencies close to 10 MHz-mm.

Furthermore, we must recall that each solution of Eq. (20) represents a superposition of propagating and standing waves of all the branches in the dispersion spectrum, which are properly combined in order to satisfy the imposed boundary conditions, and that the solution obtained with the proposed algorithm is exact,

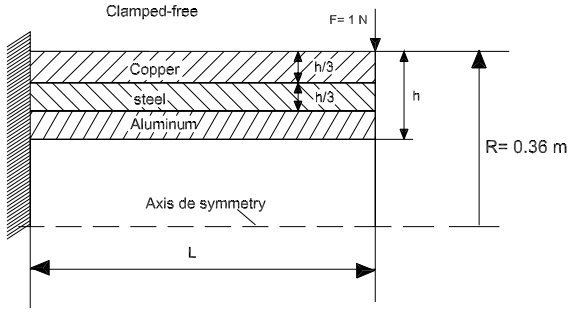

Fig. 10. Section of a clamped-free laminated cylinder ($R/h = 6$, $R/\mathrm{L} = 0.36$).

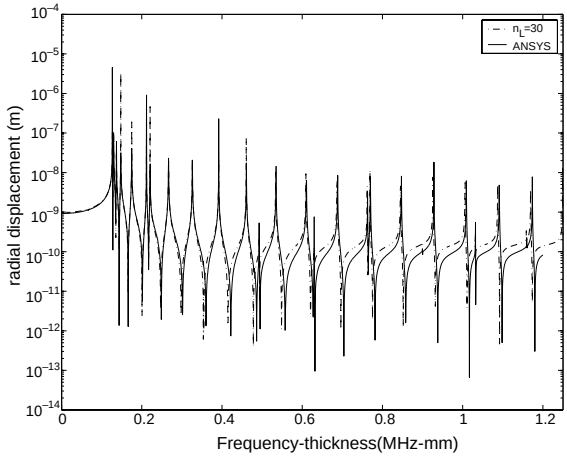

Fig. 11. Frequency response of a laminated cylinder ($n = 0$).

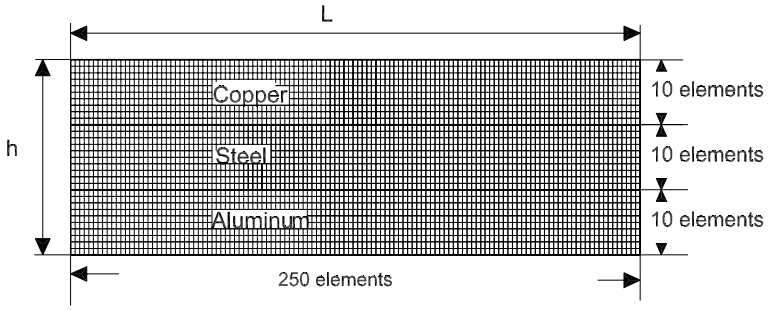

Fig. 12. Meshing of the section of a laminated cylinder ($R/h = 6$, $R/\mathrm{L} = 0.36$).

with no approximation in the axial direction. We now return our attention to Fig. 11, and verify the good correlation of results produced by both the layer-wise theory and the FEM analysis up to around the ninth natural frequency. After that, for higher frequencies and shorter wavelengths, differences between the two results start to increase. In light of the above discussion, it is reasonable to expect that results obtained with the algorithm proposed in this paper are more accurate than those from the FEM analysis of the model in Fig. 12, in particular at the high-frequency/short-wavelength range, and even though both models employ the same discretization in the radial direction.

6. Conclusion

The accuracy of layer-wise laminate shell theories in the high-frequency/short-wavelength range was investigated. A model, based on Reddy's discrete-layer theory, was developed for layered cylindrical shells. Although, in this paper, examples were presented for shells with isotropic laminae, the formulation was developed for orthotropic layers with material symmetry axes coinciding with the axial, circumferential, and radial directions. Generalization to other classes of anisotropy is straightforward. The governing equations, after considering harmonic fields, both in time and in the circumferential direction, were written in a state space form.

Evaluation of the model's accuracy in the high-frequency range was based on the frequency spectrum of free guided waves propagating in an infinite shell. Comparisons made with the exact spectrum evaluated through the theory of elasticity have demonstrated that the layer-wise model can accurately reproduce the spectrum of guided waves up to wavelengths that are much shorter than the shell thickness. Even though all comparisons were made for shells with isotropic layers, the authors believe that there is no reason not to suppose that the same conclusion would also hold for anisotropic laminated shells.

In order to solve the governing equation, we have proposed an algorithm based on a discrete version of the Riccati transformation. This approach allows one to overcome the problems associated with exponential dichotomy, which could make the solution unstable in the high-frequency range, where eigenvalues of the state matrix have large real parts. As an example, the algorithm was applied to obtain the frequency response of a laminated cylindrical shell, clamped at one end and excited by a radial axi-symmetric load at the other. These results were compared with those obtained with the aid of solid finite elements of a commercial code. Good correlation was verified up to the ninth natural frequency.

References

Abramowitz, M., Stegun, I.A., 1972. Handbook of Mathematical Functions. Nacional Bureau of Standards, Washington, DC, USA.

Braga, A.M.B., Barbone, P.E., Herrmann, G., 1990. Wave propagation in fluid-loaded laminated cylindrical shells. Applied Mechanics Reviews 43 (5, part 2), 359–365.

Braga, A.M.B., Gama, A.L., de Barros, L.P.F., 2000. Models for the high-frequency response of active piezoelectric composite beams. Journal of Applied Mechanics and Engineering 5 (1), 47–61.

Chin, R.C.Y., Hedstrom, G.W., Thigpen, L., 1984. Matrix methods in synthetic seismograms. Geophysical Journal of the Royal Astronomical Society 77, 483–502.

Dieci, L., Osborne, M.R., Russel, R.D., 1988. A Riccati transformation method for solving linear BVPs. II Computational aspects. SIAM Journal on Numerical Analysis.

Huang, K.H., Dasgupta, A., 1995. A layer-wise analysis for free vibration of thick composite cylindrical shells. Journal of Sound and Vibration 182 (2), 207–222.

Icardi, U., 1998. Cylindrical bending of laminated cylindrical shells using a modified zig-zag theory. Structural Engineering and Mechanics 6 (5), 497–516.

Lee, H.J., Saravanos, D.A., 2000. A mixed multi-field finite element formulation for thermopiezoelectric composite shells. International Journal of Solids and Structures 37 (36), 4949–4967.

Leissa, W., 1973. Vibration of Shells (NASA SP-288). US Goverment Printing Office, Washington, DC.

Loy, C.T., Lam, K.Y., 1999. Vibration of thick cylindrical shells on the basis of three-dimensional theory of elasticity. Journal of Sound and Vibration 226 (4), 719–737.

Noor, A.K., Burton, W.S., Bert, C.W., 1996. Computational models for sandwich panels and shells. Applied Mechanics Reviews 49, 155–199.

Pease, M.C., 1965. Methods of Matrix Algebra. Academic Press, New York.

Reddy, J.N., 1989. On refined computational models of composite laminates. International Journal of Numerical Methods in Engineering 27, 361–382.

Reddy, J.N., Robbins, D.H., 1994. Theories and computational models for composite laminates. Applied Mechanics 47 (6, part 1), 147–169.

Reddy, J.N., Teply, J.L., 1991. Stability of thick composite laminates using the layer-wise theory. In: Proceedings of the American Society for Composites, 6th Technical Conference, Albany, New York, pp. 289–298.